

BEHAVIOUR OF CYCLICALLY LOADED SHEAR WALLS

D. Palermo¹ and F.J. Vecchio²

ABSTRACT

Behaviour of reinforced concrete shear walls under cyclic loading is investigated. Results of a parametric study using a nonlinear finite element analysis program, performed on the NUPEC large-scale flanged shear wall, are presented underscoring the mechanisms influencing both the observed and calculated responses. Details of an ongoing experimental program on the behaviour of 3-D shear walls subjected to reversed cyclic loading are provided. The preliminary constitutive models used in the analysis programs, for reinforced concrete subjected to arbitrary loading conditions including cyclic loading, are reviewed. The analytical results of shear walls are compared to the experimentally observed behaviour, demonstrating reasonably accurate simulations of behaviour. The results of a series of panel tests are used to identify the aspects of concrete modeling that are in need of further study and refinement.

INTRODUCTION

To assess the seismic safety factor of nuclear reactor buildings, the Nuclear Power Engineering Corporation of Japan (NUPEC) conducted an extensive experimental investigation. Two large-scale flanged shear walls were subjected to dynamic loading using a high performance-shaking table. The results of the tests were made available to participants of the Seismic Shear Wall International Standard Problem (SSWISP) Workshop (NUPEC, 1996).

¹Doctoral Student, Dept. of Civil Engrg., University of Toronto, Toronto, ON, Canada, M5S 1A4

²Professor, Dept. of Civil Engrg., University of Toronto, Toronto, ON, Canada, M5S 1A4

It became evident from the competition results that current ability to predict the peak strength of shear walls under seismic excitations is not well established. More importantly, however, is the apparent inability of leading researchers to accurately predict structure ductility. The predictions received were based on FEM static monotonic and FEM static cyclic analyses, FEM dynamic analyses, simplified static and dynamic analyses, and lumped-mass dynamic analyses. Figures 1 and 2 show the analytical results of the predicted maximum load and the predicted displacement at maximum load for the FEM static models, respectively.

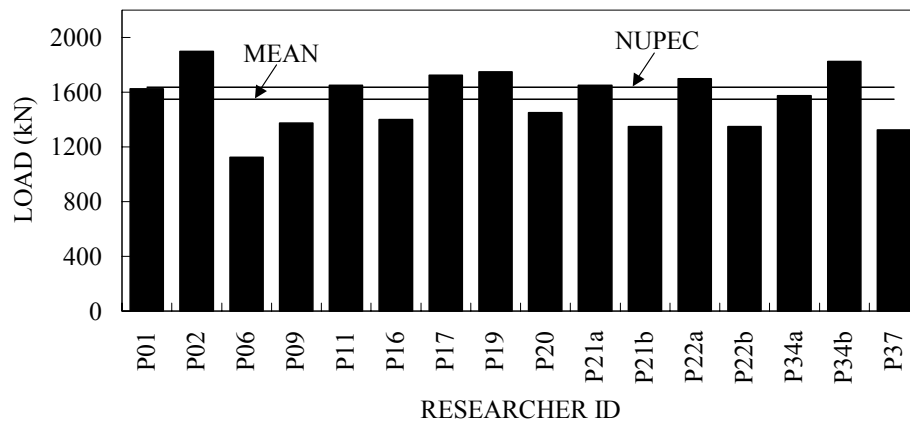


FIGURE 1. Maximum Predicted Load

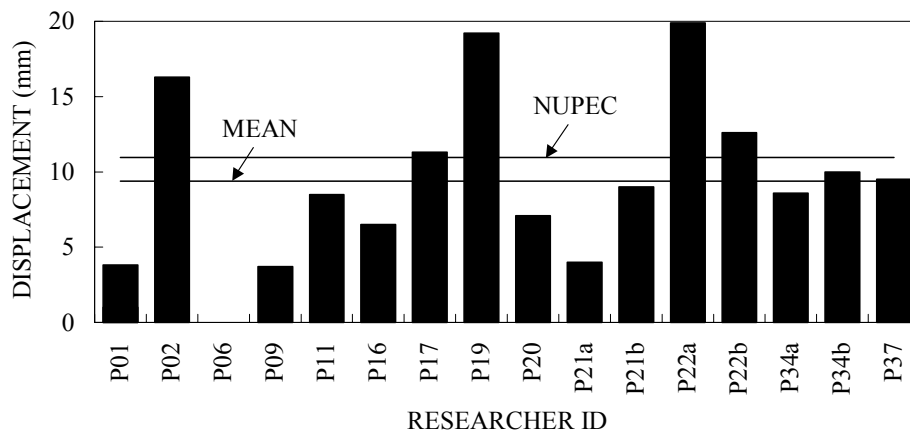


FIGURE 2. Predicted Displacement at Maximum Load

The results indicate that the methods and models used were able to predict the maximum load more accurately than the displacement at maximum load. The maximum load reported by NUPEC was 1636 kN and the corresponding displacement was 10.96 mm. The analytical maximum load results varied from 65% to 115% of the experimental value and the majority underestimated the peak strength. The variation was, however, smaller than that of the displacement at the maximum load. The range was from 35% to 180% for those participants that

submitted displacement results. Again, the majority of the predictions underestimated the ductility of the shear wall.

The inability to accurately estimate displacement indicates that significant work and attention needs to be geared towards formulating improved ductility models. Ensuring that current and future analytical models provide reasonably accurate simulations of behaviour requires experimental data to corroborate the models. Experimental data can also provide useful information into better understanding the behaviour of shear walls under cyclic loading conditions. This may include damage factors for concrete subjected to repeated cyclic loads for further softening of the concrete in compression, and the shake-out of stress in tension. The data will also lead to the formulation of more realistic unloading-reloading models.

The difficulties with predicting ductility led to large scale testing of a 3-D shear wall at the University of Toronto. The purpose of this experimental program is to investigate the behaviour of shear walls under cyclic loading, to provide test data to formulate cyclic models, and to investigate the capability to predict structure ductility using in-house FEM programs at the University of Toronto. The details of the experimental program will be discussed later.

This paper will focus on the findings to-date regarding the behaviour and analytical modeling of seismic shear walls, discuss the results of the experimental program being conducted at the University of Toronto, and describe the analytical models. The latter includes the preliminary constitutive models for reinforced concrete subjected to cyclic loading currently being employed in in-house FEM programs. The modeling of various walls will be discussed to demonstrate the reasonably accurate predictions of the current models, and future work to improve these models will be discussed.

PRELIMINARY STUDIES

A three-dimensional static nonlinear finite element analysis was performed on the NUPEC large-scale flanged shear walls that were the subject of an international competition (Vecchio, 1998). This analysis provided much insight into the behaviour of shear walls. A parametric study using a two-dimensional static nonlinear finite element analysis was later performed to further investigate the behaviour of shear walls, the factors influencing behaviour, and the factors influencing the analysis results.

Program SPARCS (Selby, 1993) was utilized for the 3-D analysis of the NUPEC specimen. This finite element program, developed at the University of Toronto, incorporates the constitutive relationships and conceptual models of the Modified Compression Field Theory. SPARCS employs a total load, secant stiffness approach in the formulation of its nonlinear analysis algorithm. The element library includes an 8-noded (24 degree of freedom) brick element, which assumes linear

displacement fields. As well, a 6-noded wedge element and a truss-bar element are available. Reinforcement is typically modeled as smeared within the elements.

The analysis performed simulated behaviour under the supposition of static monotonically increasing load. The NUPEC specimen, however, was tested under dynamic cyclically reversing loads raising some important questions that must be considered in trying to understand and correlate the predicted and observed behaviours. In the analysis, all modeling decisions were made and all the analysis parameters were set before the analysis was executed. No fine-tuning of the analysis was done to obtain a better fit of the experimental data. Shown in Figure 3 are the predicted and observed load-horizontal displacement responses of the wall.

An ultimate wall strength of 1815 kN was predicted, 12% greater than the experimentally observed value. The predicted load-deformation response agreed well with the observed behaviour before cracking; however, the cracking load and post-cracking stiffness were overestimated. Factors possibly contributing to the decreased stiffness of the specimen are the degradation of tension stiffening effects, and deterioration in the bond and anchorage of the reinforcement. Tests have indicated that, under dynamic and reversed cyclic loading conditions, reinforced concrete experiences degradation in the bond between the concrete and the reinforcement. This has the effect of diminishing the development of post-cracking tensile stresses in the concrete. The effects of bond slip can be approximated to some extent by discounting the tension stiffening effect.

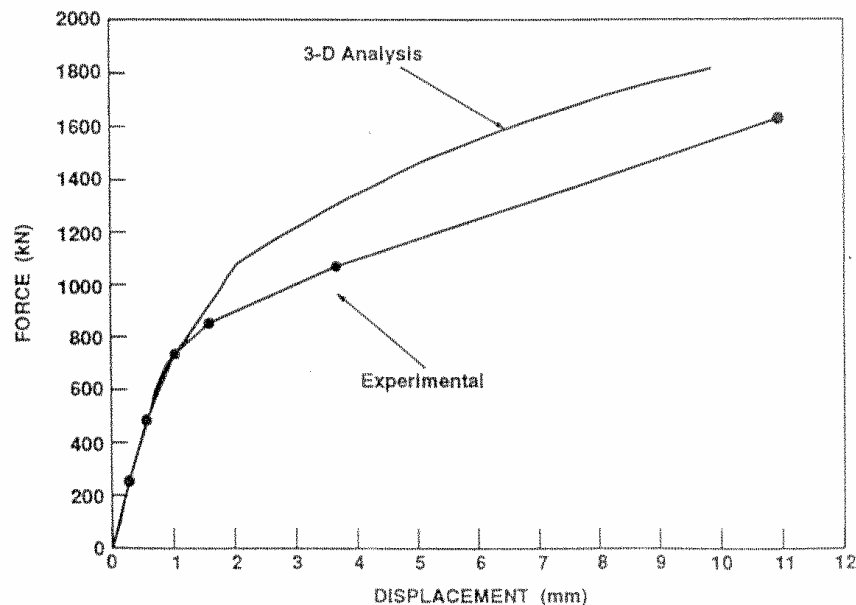


FIGURE 3. Horizontal Displacement of Top Slab

The predicted failure mode involved a shear crushing of the web, resulting in a shear plane approximately 300 mm from the base, occurring after yielding of the

reinforcement in the tension flange. This behaviour was largely in agreement with the observed failure. The sequence and location of yielding in the flange and web regions were such that ratcheting effects likely influenced the failure mode and load capacity. This phenomenon occurs when the vertical reinforcement in the flanges and near the web-flange junction yields. Once a flange yields it retains some permanent plastic strain. Upon reversing the load, the other flange is expected to yield at a similar load. Through each cycle of loading, the plastic strains resulting from yielding tend to grow. The consequence is two fold: 1) a concentrated zone of damage is created near the base, in the yield regions, leading to a potential shear plane being established; and 2) the increased strains result in a diminished confinement of the web, and an increased influence from compression softening, lowering the concrete web's ability to resist load. Thus, that the static analysis predicted a somewhat higher failure load, and a failure mode more in the nature of a shear crushing of the web, is not unexpected.

The analysis also demonstrated that three-dimensional effects are significant. The flanges are near fully effective in contributing load resistance to the structure. The massive top and bottom slabs provide out-of-plane confinement to the web wall, enhancing the strength of the adjoining concrete web elements.

Having performed and submitted analysis results based on a single analysis without fine-tuning, it became apparent that a parametric study would enhance the understanding of the behaviour and modeling of the NUPEC specimens. A two-dimensional model was used to reduce the demands on resources imposed by a three-dimensional model. Program TRIX is the equivalent two-dimensional nonlinear finite element program. It incorporates essentially the same material models and analytical formulations as SPARCS.

The parameters and models investigated include: three-dimensional effects, effective flange width, tension stiffening model, compression softening model, concrete confinement, amount of vertical reinforcement in flanges, concrete strength, and mesh size. Refer to Vecchio (1998) for a more complete discussion.

The following conclusions were determined from the parametric study:

1. Two-dimensional analyses fail to capture some important three-dimensional effects, such as the out-of-plane confinement provided by the base, and shear lag effects in the flange walls. They also lead to an overestimation of the lateral and horizontal confinement of the web provided by the flanges, and an overestimation of the contribution of the flange elements to the lateral shear stress distribution. The result was a slightly stronger and stiffer response than obtained using a three-dimensional analysis. However, the loss in accuracy was not severe, and the failure mode remained well predicted.
2. In modeling the thickness of the flange elements, four series of analyses were run, with the effective flange width modeled as 100%, 67%, 33%, and 0% effective. The strength and stiffness were greatly diminished with each

- successive reduction in width. An effective thickness of between 67% and 100% of the width of the flanges appeared to be appropriate.
3. The choice of a tension stiffening model, among several available, did not significantly affect behaviour. However, ignoring tension stiffening effects resulted in substantial increases in post-cracking deflections, and a slight lowering of the ultimate load capacity.
 4. Compression softening effects were not a significant influencing factor for the NUPEC test specimen.
 5. Confinement effects had a minor influence, resulting in a slightly increased load capacity and a positioning of the failure plane up away from the base.
 6. The amount of vertical reinforcement provided in the flanges was not a significant influencing factor; although yielding of this reinforcement immediately preceded the web shear failure.
 7. The compressive strength of the concrete in the web was fully utilized at ultimate load. Increasing or decreasing the concrete strength significantly affected the predicted failure load of the structure. Thus, the strength of the wall was most governed by the strength and thickness of the web. The vertical and horizontal reinforcement in the web was of sufficient amounts to not yield. The flanges were of sufficient width, and sufficiently reinforced, to not precipitate a flexural failure.
 8. The element mesh used to model the web wall; in both the standard two- and three-dimensional analyses were too coarse. Analytically, there was insufficient freedom for the mid-height regions of the web to overcome the restraint imposed by the stiff top and bottom slabs. A finer mesh predicted a considerably less stiff response, and a significantly lower load capacity.

EXPERIMENTAL PROGRAM

An experimental program involving large-scale flanged shear walls is underway at the University of Toronto. The aim is to investigate and better understand the behaviour of reinforced concrete under cyclic loading conditions. The database that will be available at the conclusion of testing will be used to refine the in-house analysis programs with respect to the cyclic loading models currently being employed. More accurate unloading and reloading rules will be established, and close attention will be given to post-peak ductility modeling. The ratcheting effect will also be investigated.

The experimental program consists of constructing and testing two shear walls under statically imposed cyclic displacements. The two shear walls are identical in terms of dimensions and reinforcement. The concrete strength will vary somewhat due to the fact that the walls were built at different times. To date, Part 1 of the experimental program has been completed. It consisted of testing shear wall DP1 into the post-peak range (Palermo, 1998), after which the shear wall was repaired and tested to failure (Bucci, 1998). Part 2 consists of testing shear wall DP2, repairing and further testing to failure. The difference between the two tests is the

inclusion of an imposed axial load on DP1. Details of the DP1 specimen are shown in Figure 4.

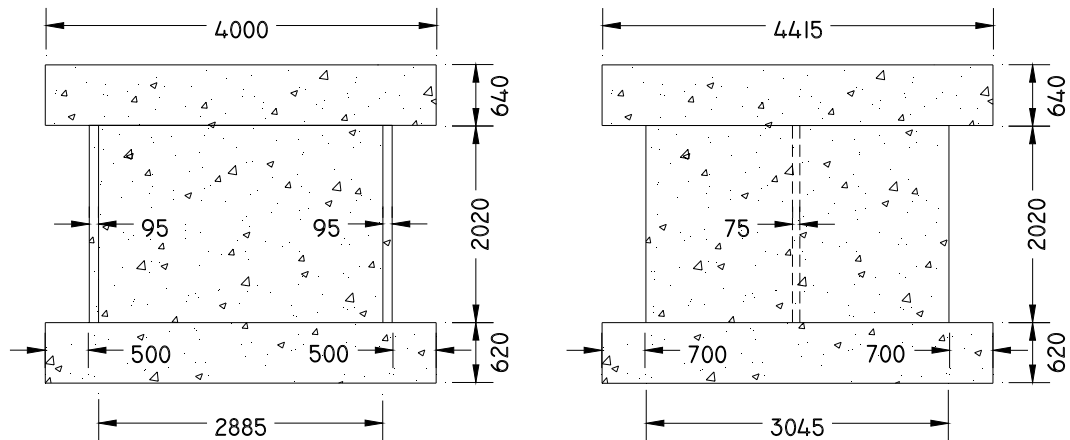


FIGURE 4. Test Specimen DP1

The two specimens are similar to the NUPEC specimens previously discussed. DP1 had stiff top and bottom slabs. The top slab (4415 mm x 4000 mm x 640 mm) served to distribute the horizontal and axial loading to the walls of the structure. The bottom slab (4415 mm x 4000 mm x 620 mm) was clamped to the laboratory floor, simulating a rigid foundation. The slabs were reinforced with No. 30 deformed reinforcing bars at a spacing of 350 mm in each direction, with a top and bottom layer. The web wall was 2885 mm in length, 2020 mm in height, and 75 mm in thickness. It was reinforced with D6 reinforcing bars. [The D6 bar has a diameter of 7 mm and a cross sectional area of 39 mm².] The reinforcing bars were placed in two layers, and spaced 140 mm horizontally and 130 mm vertically. The two flange walls were approximately 3050 mm long, 2020 mm high, and 95 mm thick. The flanges were also reinforced with D6 reinforcing bars. Horizontally, the bars were spaced at 140 mm, and vertically, the bars were spaced at 130 mm near the web wall, and 355 mm near the tips of the flanges. The concrete clear covers in the walls and slabs were 15 mm and 50 mm, respectively.

The concrete cylinder strengths of the walls, top slab, and bottom slab were 22 MPa, 44 MPa, and 35 MPa, respectively. The corresponding strains at peak strengths were 2.0×10^{-3} , 1.9×10^{-3} , and 1.7×10^{-3} , respectively. The D6 reinforcing bar had a yield strength of 605 MPa, with a corresponding yield strain of 3.2×10^{-3} , an ultimate strength of 652 MPa corresponding to a rupture strain of 88.3×10^{-3} , and Young's Modulus of 200 000 MPa. The No. 30 reinforcing bar had a yield strength of 550 MPa at a strain of 2.5×10^{-3} . The ultimate strength was 696 MPa, and Young's Modulus was 220 000 MPa.

Loading of DP1 consisted of increasing horizontal cyclic displacements applied to the top slab, combined with a constant axial load of 1200 kN. The axial load consisted of a 260 kN contribution from the self-weight of the top slab and a 940 kN

contribution of applied loading. Imposed displacements in increments of 1 mm, with two repetitions at each displacement level, were applied in the horizontal direction, along the axis of the web wall. Two actuators, mounted to the laboratory strong wall and connected to the top slab of the specimen, introduced the displacements. Testing was terminated after imposing 15 mm of displacement, after which the structure was repaired and tested to failure. The specimen was mounted with 40 strain gauges, measuring reinforcement strains; 62 Zurich targets, measuring concrete surface strains; and 21 LVDTs, measuring horizontal and vertical displacements. Figures 5 and 6 are photos of DP1 at peak load and at failure, respectively.

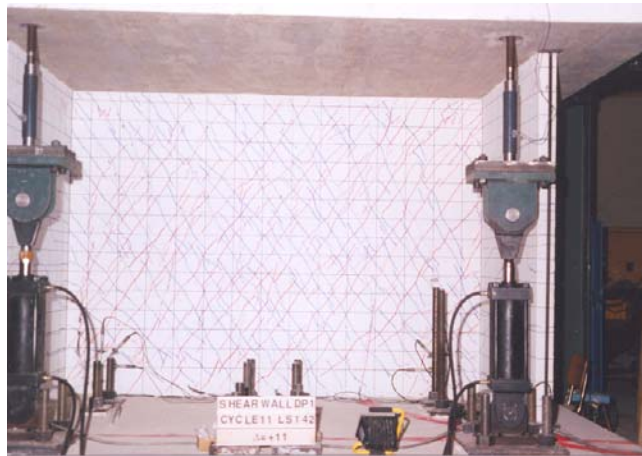


FIGURE 5. DP1 at Peak Load

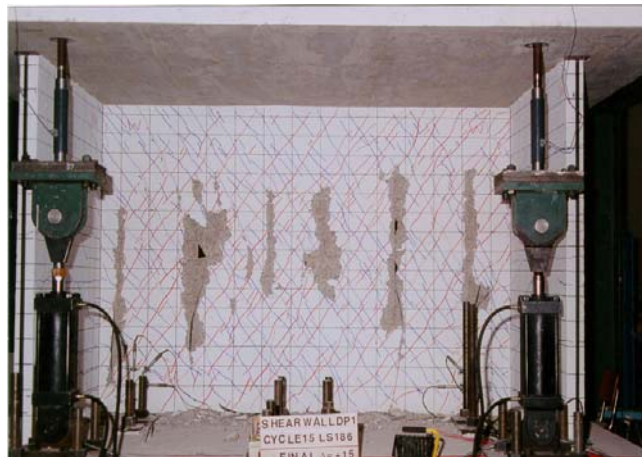


FIGURE 6. DP1 at Failure

Cracking first surfaced on the web wall at a load of -408 kN and a corresponding displacement of -0.6 mm. This shear crack formed during the first excursion to -1 mm; negative referring to pulling of the specimen toward the strong wall. By the

end of cycle 4 (4 mm of displacement), the web wall was essentially fully cracked on both faces. The maximum shear crack width was 1.0 mm and it was recorded during cycle 13 and beyond. The shear cracks were approximately inclined at an angle of 45 degrees to the horizontal. The first flexural crack appeared during the first excursion to 3 mm, on the outside surface of the flange farthest from the strong wall. The approximate load and displacement at the onset of cracking was -819 kN and -2.9 mm, respectively. The maximum flexural crack width of 1.1 mm was recorded during the first excursion to 12 mm of displacement.

Testing was terminated after the completion of cycle 15, at which point a significant portion of the descending branch of the load-deformation response had been attained. The maximum loads were recorded in the first excursion to 11 mm, in both the positive and negative directions. The maximum load and corresponding displacement for the positive cycle were 1298 kN and 11.1 mm, respectively, -1255 kN and -11.1 mm for the negative cycle. At the onset of cracking, the structure began to retain a permanent deformation. At the end of testing, a permanent deformation of 3.3 mm was recorded. The load-deformation response of DP1 is shown in Figure 7. The response shows that the structure was in its post-peak response after 11 mm of displacement. The second excursion for each cycle produced hystereses of reduced stiffness and peak strength. Important trends that were determined from the response curves include: 1) the unloading curves of the second excursions of a displacement amplitude followed the unloading curves of the first excursion for the same amplitude; and 2) the loading curves of subsequent displacements for the first excursion followed the loading path of the second excursion of the previous displacement. These trends continued until the peak load, after which the structure deviated from this behaviour.

The strain gauges used to measure reinforcement strains indicated that only the horizontal rebars in the web wall near mid-height had yielded. The gauges did not indicate yielding in the flexural reinforcement; however, the concrete surface gauges recorded surface strains in excess of yielding, suggesting that there was some local yielding of the flexural reinforcement in the flanges.

At the end of testing, six vertical planes of failure, equally spaced along the web wall, were visible. These planes began to form during 11 mm of displacement, near the toes of the web. At this point, the structure was in its post-peak range. The concrete within the web experienced widespread damage and its ability to contribute significantly to resisting the horizontal displacements was impaired. With each successive cycle beyond 11 mm, the integrity of the concrete continued to diminish. Failure, ultimately, involved severe crushing of the concrete over a widespread region of the web wall.

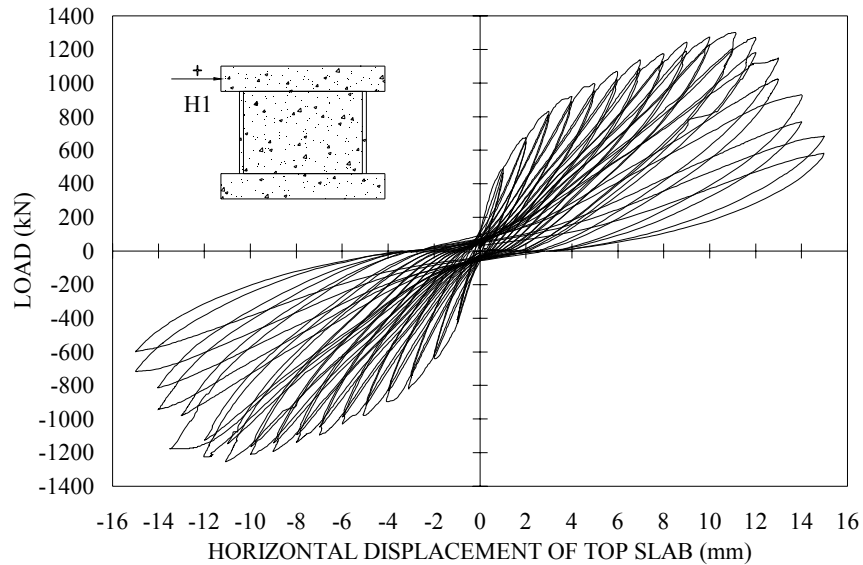


FIGURE 7. Observed Load-Deformation Response of DP1

Testing was terminated at 15 mm of displacement so that a simple and conventional repair strategy could be applied. At the time of repair, an assessment of the damage was performed visually and by examining the experimental data. The concrete in the web appeared thoroughly crushed and was marked by vertical planes of weakness. In the later load stages, the greater part of the concrete experiencing crushing occurred along these vertical planes. The flanges experienced flexural cracking; otherwise no other significant damage was evident. The vertical reinforcement in the web wall seemed not to have undergone plastic deformations, and was deemed to be within the elastic phase. Conversely, the horizontal rebars appeared to have yielded uniformly along their length. The vertical reinforcement in the flanges had yielded only locally, in the proximity of cracks, while the horizontal rebars remained undamaged. All structural joints connecting the walls with the top and bottom slabs were judged to be in good condition.

As a consequence of the assessment, it was decided to rehabilitate the structure by removing all the concrete in the web area, with the exception of a 50 mm sound layer of concrete at the construction joints. New concrete and a top layer of grout replaced the damaged concrete. The reinforcing steel was left in place. The flange walls remained in their damaged state from the original test.

The material properties of the structure remained unchanged except for the new concrete cast into the web wall. The concrete had a strength of 44 MPa and the grout 50 MPa on the day of testing. The goal was to achieve similar strengths to that of the original wall; however, a delay in testing caused an increase in the strength of the concrete.

The testing apparatus and instrumentation was identical to the first test. Loading was applied in the exact manner as in the original test. Two cyclic repetitions for

each displacement level were imposed. The displacements were incremented by 1 mm, and testing was terminated at 17 mm when failure was visibly evident. Figure 8 shows the state of DP1-R at failure.

The first crack surfaced in the web wall at a load of -133 kN and a corresponding displacement of -0.3 mm. Shear cracks continued to surface in the web with increasing displacement, and were approximately inclined at 45 degrees to the horizontal. The maximum crack width measured in the web was 0.6 mm. No new flexural cracks in the flanges were reported. Figure 9 gives the load-deformation response of the repaired specimen.



FIGURE 8. DP1-R at Failure

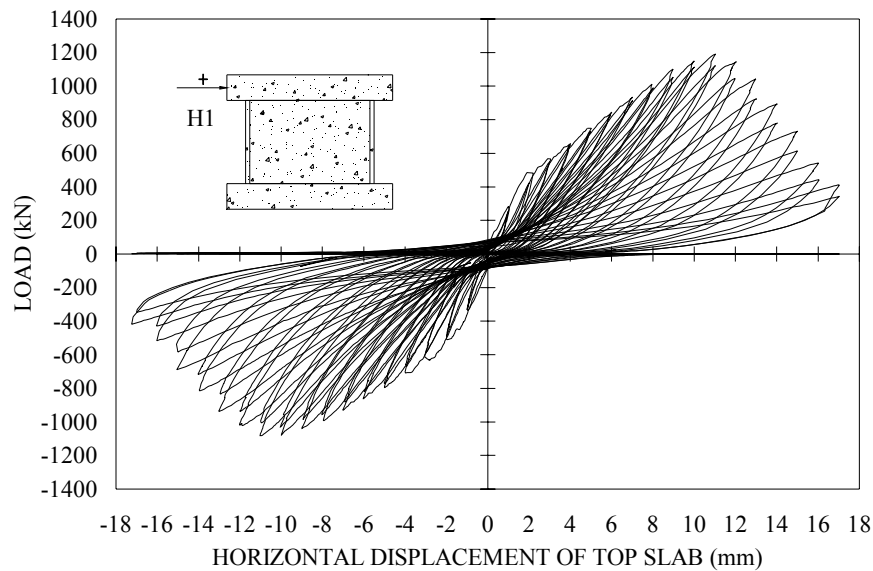


FIGURE 9. Observed Load-Deformation Response of Repaired DP1

The peak loads were recorded during cycle 11 for both the positive and negative directions. In the negative direction, the maximum load attained was -1192 kN at a displacement of -11 mm, 1081 kN corresponding to a displacement of 11 mm for the positive direction. The repaired structure was able to restore 92% of its original strength. The response indicates that the structure was in its post-peak range beyond 11 mm of displacement, and testing was terminated after the completion of cycle 17. At this stage, failure was evident in the form of concrete crushing near the toes of the web and a punching of the flange at the intersection with the web wall. A shear sliding plane of damage was apparent at the web-base intersection. No yielding of the reinforcement was recorded by the strain gauges that remained functional after the first test.

ANALYTICAL MODEL

Vecchio (1999) proposed an analytical model for reinforced concrete subjected to cyclic loading. The constitutive models for concrete in compression and tension are provisional and further work is required in this area. The hysteretic model for reinforcement has been modeled after Seckin (1981). Analyses using these models confirm that the procedure provides accurate simulations of behaviour.

The formulations of this procedure are such that a secant stiffness-based algorithm, employing the smeared rotating crack assumption, can be adapted to represent hysteretic material response under general loading and reversed cyclic loading. The procedure follows the approach proposed by Vecchio (1992), which accounts for prestrains in the finite element procedure. The total strain at any point in the concrete can be considered to consist of an elastic strain component and a plastic strain component. The elastic strain can be used to compute effective secant stiffness for the concrete. The plastic strain, however, must be treated as a strain offset similar to other prestrain effects. The plastic offsets in the principal directions are resolved into components relative to the reference axes. From the prestrains, free joint displacements are determined. Then the plastic prestrain nodal forces can be evaluated using the effective element stiffness matrix due to the concrete component. The plastic offsets in each reinforcement component are handled in a similar manner. The total nodal forces for the element can be calculated as the sum of the concrete and reinforcement contributions. These are added to prestrain forces arising from elastic prestrain effects and from nonlinear expansion effects.

A Mohr's circle is used to provide a simple means of tracking the plastic offsets that are to be used in the concrete constitutive models. These parameters defining the envelope of plastic strains can be updated as further plastic straining occurs from the increments in the plastic strains in the principal directions. A Mohr's circle of construction is also used to approximate the maximum strains in the principal directions used to describe the backbone curve of the hysteretic concrete model.

The maximum strains are updated if the current total strains are greater than those previously recorded.

The proposed concrete models essentially use linear unloading/reloading rules for simplicity. The base curve describing the monotonic concrete compressive response is based on a Hognestad parabola or Popovics formulation, modified to account for compression softening effects according to the Modified Compression Field Theory. Figures 10 and 11 describe the hysteresis model for concrete in compression and tension, respectively. Refer to Vecchio (1999) for the hysteresis formulations.

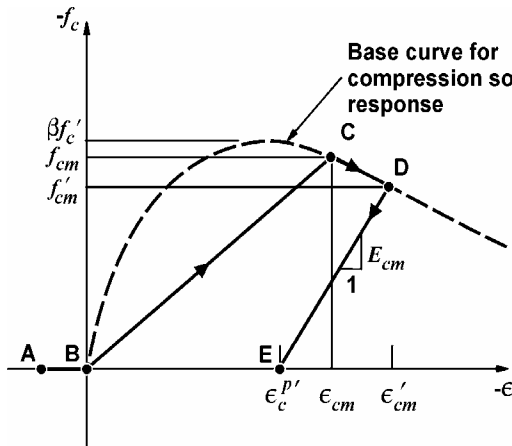


FIGURE 10. Compression Model

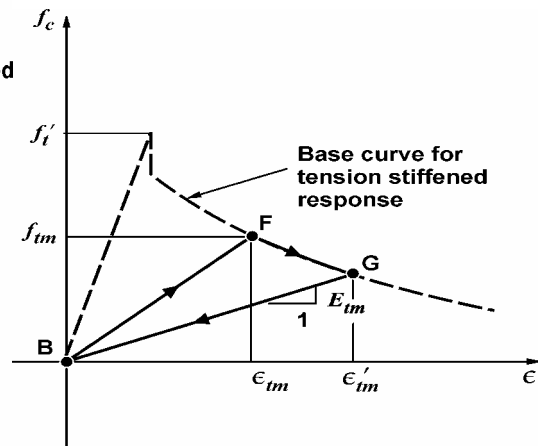


FIGURE 11. Tension Model

A nonlinear unloading branch for concrete in compression and tension has been incorporated into the formulations since.

The monotonic stress-strain response of reinforcement is assumed to be tri-linear. The reloading and hysteretic response of the reinforcement is modeled after Seckin (1981). The Bauschinger effect is represented by a Ramberg-Osgood formulation.

CORROBORATION

Analyses of a series of large-scale shear walls were undertaken to obtain a preliminary indication of the suitability of the proposed approach to cyclic response modeling of reinforced concrete (Lai, 1998). Further analyses were performed on a series of reinforced concrete panels to assess the microscopic behaviour, such as localized damage, failure modes, and failure loads in shear or compression. In each case, the nonlinear hysteresis model for concrete was utilized.

Using program TRIX, shear wall analyses consisted of modeling four PCA wall specimens, B1, B2, B7, and B8 (Oesterle, R.G., et. al., 1976), and University of Toronto specimen DP1. The PCA specimens consisted of identical geometric properties, but varying amounts of web reinforcement, concrete confinement, and

axial load. The results fairly accurately predicted the ultimate strengths, load-deformation responses, and failure modes. In general, the analyses overestimated the energy dissipation of the shear walls. The experimental results produced a more pinched hysteresis loop. In each case, except for B2-2, tension stiffening was considered in the analysis, contributing to an overestimation of the dissipated energy. Table 1 summarizes the experimental and analytical results, and Figure 12 shows the predicted load-deformation response of DP1.

TABLE 1. Experimental vs. Analytical Results

<i>SPECIMEN</i>	F_{exp}	F_{pre}	F_{exp}/F_{pre}
B1	276	287	0.96
B2	685	709	0.97
B2-2	685	682	1.00
B7	999	1023	0.98
B8	959	1009	0.95
DP1	1298	1294	1.00

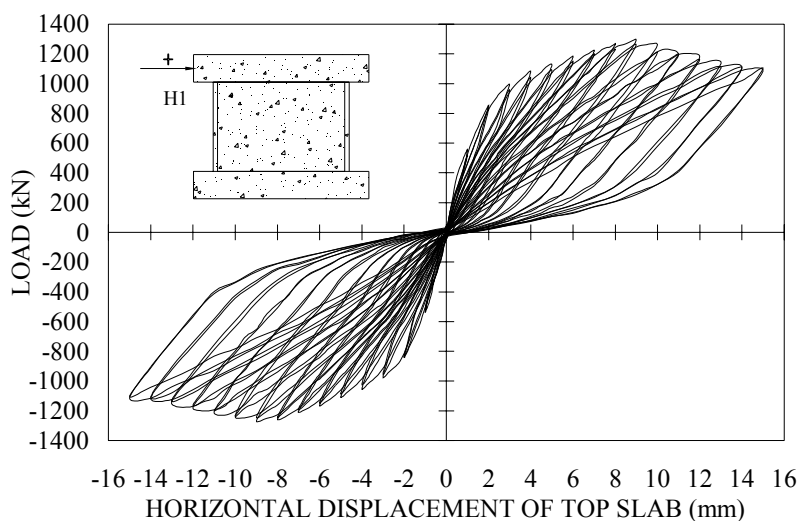


FIGURE 12. Predicted Load-Deformation Response of DP1

Figures 13 and 14 depict the experimental and analytical results of PCA specimen B2. The calculated response shown (B2-2) ignored tension stiffening effects and used the nonlinear unloading hysteresis model for concrete. The predicted to experimental failure load ratio was one. The correlation is reasonably good with respect to the wall's lateral resistance, the onset of failure, residual deflections upon unloading, and the degradation of the lateral stiffness with increased displacements. The only notable discrepancy between the calculated and observed behaviour is the

degree of pinching. This is likely related to the shape of the base hysteretic models used for the compression and tension responses.

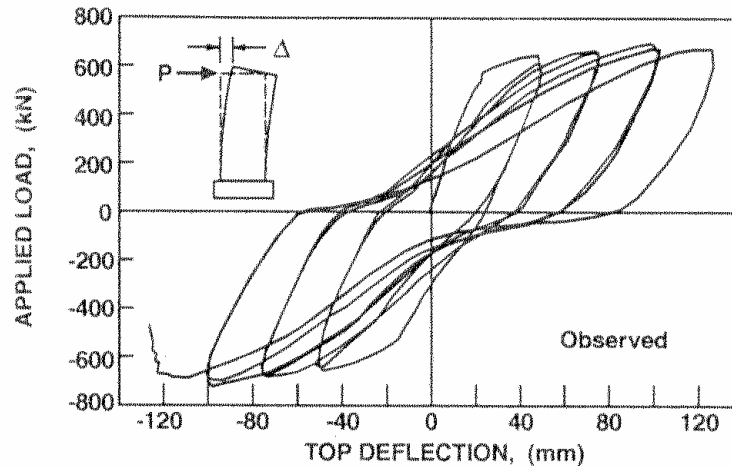


FIGURE 13. PCA B2 Experimental Results

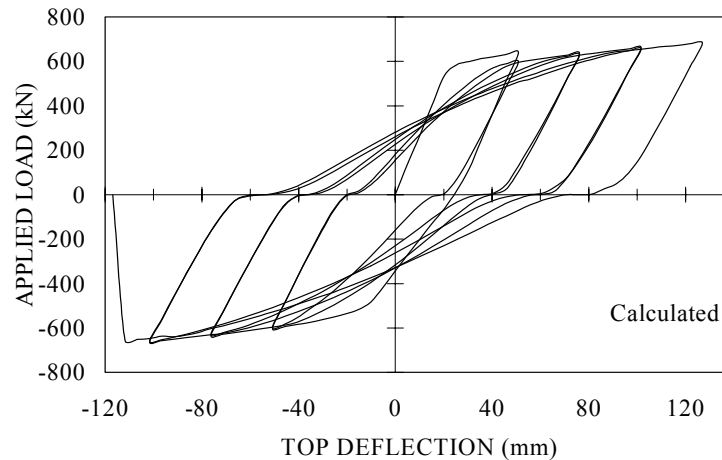


FIGURE 14. PCA B2 Analytical Results

To test the fundamental constitutive behaviour of reinforced concrete, under various loading conditions, analyses were conducted on simple reinforced concrete panels tested at the University of Toronto (Villani, 1995). The objective of this work was to accumulate the necessary data to more accurately define the hysteretic models for cracked reinforced concrete in compression and in tension, under general loading conditions.

The experimental program involved three 890 x 890 x 70 mm orthogonally reinforced panels constructed of normal strength concrete. The panels contained 1.82 percent reinforcement in one direction and 0.91 percent in the perpendicular direction. The reinforcement had a nominal diameter of 6 mm, and a yield strength of 282 MPa. The panels were loaded under conditions of biaxial compression and shear in the fixed proportion of $f_{n_x}:f_{n_y}:v = -0.4:-0.4:1.0$.

Panel PDV2, subjected to reversed cyclic shear, was constructed from concrete having a peak strength of 23.7 MPa. PDV2 failed by shear failure of the concrete occurring almost coincidentally with yielding of the reinforcement in the x-direction. The reinforcement in the y-direction yielded well before failure.

The test panel was analyzed with program TRIX using the nonlinear hysteretic model for concrete. It was found that failure ultimately occurred when the reinforcement in x-direction yielded. The reinforcement in the y-direction had yielded well before failure. The concrete at the time of failure was in its post-peak range and experiencing shear crushing. The experimental and analytical responses are shown in Figures 15 and 16, respectively.

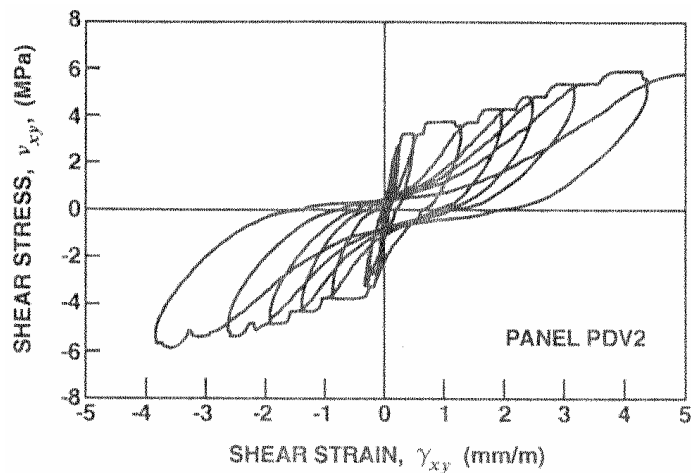


FIGURE 15. PDV2 Experimental Results

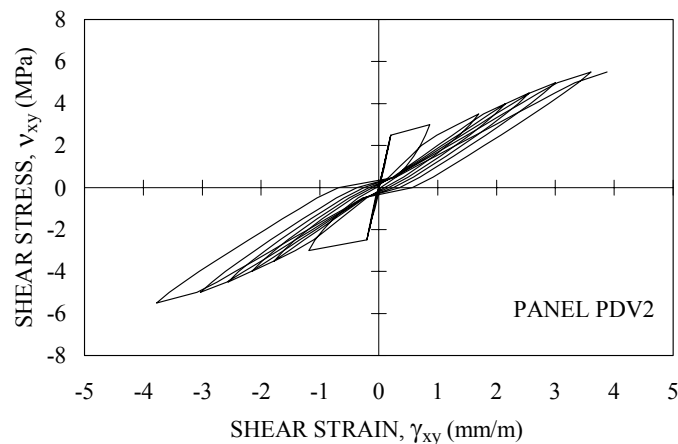


FIGURE 16. PDV2 Analytical Results

The experimental response demonstrates a behaviour more influenced by concrete shear failure. Upon unloading, the stiffness is substantially lower and the residual strains are significantly larger. The damage to the concrete is more extensive than that assumed in the models and is evident when examining the principal

compressive and principal tensile stress-strain behaviour. The analysis indicates that improvements are required to the nonlinear hysteretic models for concrete subjected to cyclic loads.

CONCLUSION AND FUTURE WORK

This paper has focused on the behaviour of reinforced concrete subjected to reversed cyclic loading conditions. Through analysis with three-dimensional and two-dimensional finite element programs, and extensive experimental data, a better understanding of the behaviour has been possible.

Limitations in analysis are a direct result of the suitability of constitutive models for concrete under cyclic loading. Generally, two-dimensional analyses predict the load-deformation of structures fairly accurately; however, they fail to capture some important three-dimensional effects such as the out-of-plane confinement and shear lag effects. Two-dimensional analyses also tend to overestimate contributions of out-of-plane elements to the lateral resistance of a structure. The loss in accuracy, due to the above deficiencies, is not severe.

Preliminary constitutive models have been proposed for concrete, and analyses have shown the procedure to be compliant and to provide reasonably accurate simulations of behaviour. However, the paper has also identified areas where improvements can be made.

An extensive experimental investigation is currently underway at the University of Toronto. The results will be used to further corroborate and modify the cyclic models for concrete. They will also be used to investigate other effects of reinforced concrete subjected to cyclic loading, namely: the ratcheting effect of the reinforcement; the influence of bond slip, which has the effect of diminishing the development of post-cracking tensile stresses in the concrete; the influence of cyclic load damage on concrete, which has the effect of increasing the compression softening effect; and the influence of crack slip, which is used as a check to ensure that local stresses in the reinforcement can be tolerated at a crack location. In the proposed model, the compressive stresses remain zero until the cracks completely close in an excursion returning from the tensile strain domain. Experimental evidence, however, suggests that the re-contact strain will be somewhat greater than zero and will be influenced by the crack shear slip.

The experimental program has also demonstrated that a full depth repair of the concrete in a shear wall can be an effective repair strategy.

REFERENCES

- Bucci, F. (1998). "Finite Element Analysis of Repaired Concrete Structures." MASC thesis, Department of Civil Engineering, University of Toronto, 158 pp.
- Lai, D. (1998). "Nonlinear Finite Element Analysis of Shear Walls Subjected to Cyclic Loads." BASC thesis, Department of Civil Engineering, University of Toronto, 70 pp.
- Nuclear Power Engineering Corporation (1996). "Comparison Report, Seismic Shear Wall ISP, NUPEC's Seismic Ultimate Dynamic Response Test." Report No. NU-SSWISP-D014, Organization For Economic Co-Operation and Development, Paris, 407 pp.
- Oesterle, R. G. et al. (1976). "Earthquake-Resistant Structural Walls-Test of Isolated Walls." Report to the National Science Foundation, Construction Technology Laboratories, Portland Cement Association, Skokie, Ill., 315 pp.
- Palermo, D. (1998). "Testing of a 3-D Shear Wall Under Cyclic Loading." MASC thesis, Department of Civil Engineering, University of Toronto, 240 pp.
- Seckin, M. (1981). "Hysteretic Behaviour of Cast-in-Place Exterior Beam-Column-Slab Subassemblies." PhD thesis, Department of Civil Engineering, University of Toronto, 266 pp.
- Selby, R. G. (1993). "Three-Dimensional Constitutive Relations for Reinforced Concrete." Publication No. 93-02, Department of Civil Engineering, University of Toronto, 147 pp.
- Vecchio, F. J. (1992). "Finite Element Modeling of Concrete Expansion and Confinement." *Journal of Structural Engineering*, ASCE, 118 (9), 2390-2406.
- Vecchio, F. J. (1998). "Lessons From The Analysis of a 3-D Concrete Shear Wall." *Structural Engineering and Mechanics*, 6 (4), 439-455.
- Vecchio, F. J. (1999). "Towards Cyclic Load Modeling of Reinforced Concrete." *ACI Structural Journal*, 96 (2), 193-202.
- Villani, D. R. (1995). "Reinforced Concrete Subjected to Cyclic Loads: A Pilot Study." BASC thesis, Department of Civil Engineering, University of Toronto, 147 pp.